Biomass Conversion and Biorefinery
https://doi.org/10.1007/s13399-021-02053-0

ORIGINAL ARTICLE

Sherry wine industry by-product as potential biosorbent for the removal of Cr(VI) from aqueous medium

L. Sánchez-Ponce[1] · M. D. Granado-Castro[1] · M. J. Casanueva-Marenco[1] · M. D. Galindo-Riaño[1] · M. Díaz-de-Alba[1]

Received: 3 August 2021 / Revised: 30 September 2021 / Accepted: 17 October 2021

Abstract

A low-cost biosorbent obtained from the Palomino Fino grape seed, a Sherry wine industry by-product, has been proposed as a way of valorising this material. The biomass was characterised obtaining values of 0.68 ± 0.05 g mL^{-1} for bulk density, 1.02 ± 0.09 g mL^{-1} for apparent density and 33.3% for porosity. The pH_{pzc} was 5.2 and the surface negative charge value was 2.4 ± 0.2 mmol g^{-1}. The analysis of surface morphology showed differences due to the sorption. The results showed a promising potential for chromium(VI) removal from aqueous solutions. The studies were carried out in batch scale and a 2^3 factorial design was applied for the optimisation of the process. A percentage of 91.7 ± 0.6% was achieved for the biosorption of Cr(VI) under optimal conditions using pH 5.5, 15 g/L of biosorbent and 8 h of contact time. The biosorption capacity showed a remarkable linearity from 0 to 2 mmol L^{-1} Cr(VI) and a precision of 0.64% for the removal of 1 mmol L^{-1} of metal. Langmuir, Freundlich and Temkin isotherm equations and the parameters of six kinetic models were used in the equilibrium modelling and identifying the mechanism of the biosorption. The combination of physical and chemical sorption mechanisms was proposed for the chromium removal with a high maximum sorption capacity ($q_{max} = 208.3$ mg g^{-1}). Thermodynamic parameters indicated the spontaneous and endothermic nature of the chromium removal. The successful biosorption was based on the special grape seed components with a relevant content in antioxidant and lignocellulosic compounds.

Keywords Chromium(VI) removal · Biosorption · Agricultural by-product · Grape seed · Non-living biomass

1 Introduction

Water pollution is a serious global problem which can lead to serious consequences for both the environment and human health. The discharge of untreated industrial effluents into aquatic ecosystems has generated the need to remove organic and inorganic water pollutants. Heavy metals are one of the most important water pollutants due to their non-degradability, toxicity and bioaccumulation tendency, facilitating their inclusion and long persistence in the food chain [1]. Thus, many methods have been applied for heavy metal removal from water and wastewater such as solvent extraction, osmosis, ion exchange, membrane filtration, chemical precipitation, coagulation/flocculation or electrochemical treatment technologies. These conventional methods can present some disadvantages in terms of applicability, high operational costs, high amounts of chemical reagents, production of hazardous wastes, high energy consumption, etc. [2, 3].

Sorption methods can be an interesting alternative in the removal of pollutants from contaminated waters. Activated carbon has shown great properties as heavy metal sorbent but the high cost of the activation process limits its use [4, 5]. Therefore, different approaches have been studied for the development of cheaper and effective metal sorbents such as biological substrates [6, 7]. Biosorption, defined as the process of ions binding from aqueous solution to biological materials, has become an eco-friendly alternative to conventional methods offering advantages such as reduction in the use of chemicals, energy, time and cost of analyses [8]. Metal ions are retained on surfaces and active sites of biosorbents. The most common biological materials used are plant biomass or microorganisms with their cell wall as the main biosorption site [7]. The application of dead biomass is preferred over living organisms due to several advantages: (i) absence of toxicity limitations; (ii) the economic aspects relating to nutrient supply and growth maintenance; (iii)

✉ M. D. Galindo-Riaño
dolores.galindo@uca.es

[1] Department of Analytical Chemistry, Institute of Biomolecules (INBIO), Faculty of Science, CEI-MAR, University of Cadiz, Cadiz, Spain

Published online: 09 November 2021

easy absorbance and recovery of metals after biosorption; (iv) easy biomass regeneration and reuse; (v) easier mathematical modelling of metal uptake; and (vi) more functional groups to participate in the biosorption process [9]. Thus, non-living biomass (such as algae, aquatic ferns, lichens, agricultural by-products and wastes) has been applied as potential biosorbents in the same way as synthetic sorbents for the removal of heavy metals from wastewaters [3].

Several factors can affect the effectiveness of the biosorption as the chemical properties of the target metal (ion mass, ionic radius and oxidation state), the characteristics of the selected biomass (types and number of binding sites, spatial distribution and accessibility to functional groups for metal ions, the affinity of binding sites for metal ions, particle size of biomass, surface morphology, chemical modification of biosorbent, etc.) and the experimental conditions of the process (pH, temperature, ionic strength, contact time, biomass dosage, metal concentration in the feed solution, competitive sorption among different metal ions, etc.) [7, 10].

A huge interest has been focused on the study of agricultural by-products or residues as low-cost biosorbents [11]. Agricultural by-products and wastes are abundant, easily available and inexpensive. They have a loose surface, porous structure and chemical stability and contain a range of different reactive functional groups (mainly carboxyl and phenolic functional groups). All these properties make them particularly interesting to be used as biosorbents [7, 12, 13]. Coffee and tea residues, sugarcane or sorghum bagasse, sugar beet pulp, waste pomace of olive oil factory waste, rice and wheat straw, fruit and vegetable peels, grape wastes and other types of biomass have been utilised as low-cost sorbents for the removal of heavy metals from wastewater [11, 14]. These materials are readily available in large quantities, and limited technology and expertise are required to integrate these materials into a water treatment process. In developed countries, agricultural and industrial wastes can be regarded as a source of abundant and effective sorbents for water treatment processes [15].

Chromium (Cr) is the twenty-first most abundant element in nature. The most common states found in the environment are the metallic (Cr(0)), trivalent (Cr(III)) and hexavalent (Cr(VI)). Cr(0) is mainly in its metallic form as a component of iron-based alloys (such as stainless steel); Cr(III) is naturally present in rocks and soils and can be easily assimilated by plants; and Cr(VI) stems largely from industrial processes, is highly soluble in water and remains stable under oxidising conditions with significant mobility through soils and aquifers.

This element occurs in many industrial effluents from leather, textile, tanning, glass and electroplating industries as Cr(III) and Cr(VI) available. Thus, it is one of the main pollutants in surface water and groundwater, being Cr(VI) about 500 times more harmful than Cr(III) [7, 16]. The Cr(III)/Cr(VI) relation depends on the pH value and the oxidative properties of the aqueous system. There is evidence that a dietary intake of Cr(III) is not essential for human life and to consider it as a nutritional supplement is often questioned. On the other hand, an exposure to Cr(VI) can lead to toxic and carcinogenic effects including oxidative stress, epigenetic changes, chromosome and DNA damages and mutagenesis [17]. Low-cost biomaterials as aquatic and terrestrial plants as well as waste materials, especially agricultural and agricultural-related industry wastes, have been used to remove different heavy metals from water sources, such as chromium [3, 11, 18].

In the present work, a locally available residue, Palomino Fino grape seed, from the world-famous and important Spanish Sherry wine industry, has been applied for the first time as a low-cost biosorbent. The Jerez area (in the south of Spain) has been traditionally involved in high-quality Sherry wine production, known as Jerez-Xérès-Sherry PDO (protected designation of origin) region. Different white wines, such as *fino*, *amontillado*, *oloroso*, *palo cortado* or *manzanilla*, are produced using this grape variety. Wine industry produces large amounts of waste from which grape seeds account around 38–52% of the solid wastes generated [19]. The winery waste is rich in lignocellulosic compounds with significant active functional groups. In particular, grape seeds are mainly composed of 40% fibres, 10–20% oil, 10–11% proteins, 7% phenolic compounds and other compounds as sugars, vitamins or minerals [19, 20]. Tocopherols are one of the most powerful natural fat-soluble antioxidants present in grape seeds influenced by harvest conditions [21]. Fibres comprise mainly insoluble compounds like cellulose and lignin and a less content of soluble fibre (hemicelluloses and pectins). Grape seed oil mostly consists of triglycerides (TG), which are rich in unsaturated fatty acids. The Fine Palomino grape seed has a high fat content, especially in linoleic and oleic acid, being low in saturated fatty acids. It is found inside the seed so it is not affected by the crushing process [22]. Flavonoids stand out among the phenolic compounds of grape seeds as well as phenolic acid, tannins and other natural antioxidants such as tocopherols; resveratrol, catechin, epicatechin, gallic acid and particularly tannic compounds, among others, are found in grape seed [23]. It is known the antioxidant potential of these compounds based on their structure with ability for radical scavenging, electron donation or chelation of metal ions [24]. This composition of seeds provides potential sorption sites of great interest for heavy metal ions. Therefore, the biomass obtained from Palomino Fino grape seeds was selected in this paper to valorise this residue (produced in large amounts and easily available at no additional cost) for the removal of Cr(VI) from water sources.

2 Experimental

2.1 Reagents and instrumentation

Milli-Q deionised water (Millipore, USA) was used for the preparation of aqueous solutions. The natural fats and oils were extracted from the biomass with n-hexane (hexane mixture of isomers RS for HPLC-isocratic grade, Carlo Erba, Spain). To determine the pH value at the point of zero charge (pH_{pzc}) and the surface negative charge of the biomass, sodium chloride (NaCl pro analysis, Panreac, Spain), sodium hydroxide (NaOH, pro analysis, Panreac, Spain) and hydrochloric acid (HCl 37% wt., pro analysis, Panreac, Spain) were used; potassium hydrogen phthalate ($KC_8H_5O_4$, pro analysis, Panreac, Spain) was used for the standardisation of NaOH solutions used. Iodine (0.01 mol L^{-1} I_2 solution, pro analysis, Panreac, Spain), sodium thiosulfate pentahydrate ($Na_2S_2O_3{\cdot}5H_2O$, pro analysis, Panreac, Spain) and starch ($(C_6H_{10}O_5)_n$ 1% wt. solution, Panreac, Spain) were employed in the iodine adsorption capacity determination; thiosulfate solutions were standardised using potassium dichromate ($K_2Cr_2O_7$, pro analysis, Merck, Germany) and potassium iodide (KI, pro analysis, Scharlau, Spain).

The sorption process was carried out using $K_2Cr_2O_7$ salt (100%, pro analysis, Merck, Germany) as metal ion precursor. The pH values of aqueous solutions in batch experiments were adjusted with CH_3COOH/CH_3COONa buffer at a final concentration of 0.1 mol L^{-1} and prepared by adding sodium hydroxide (NaOH, pro analysis, Panreac, Spain) to the acetic acid (CH_3COOH 96%, pro analysis, Merck, Germany) solution; HCl and NaOH solutions were used for preliminary experiments. Stock aqueous solutions of Cr(VI) for the calibration curve were prepared from an ICP standard solution of 1000 mg L^{-1} (in 0.5 mol L^{-1} HNO_3, Certipur, Merck, Germany) and acidified with 2 mL L^{-1} HNO_3 (Suprapur grade, Merck, Germany).

A ZM 200 cryogenic grinding (Retsch GmbH, Germany) was used to efficiently grind the Palomino Fino grape seeds. The pH measurements were carried out using a Basic 20 pH-meter with a 50_10T combined glass-Ag/AgCl electrode (Crison, Spain). Sorption experiments were performed using an HS 501 D open air laboratory shaker platform (Ika, Labortechnik, Germany). The mixture of biosorbent and solution was filtered on a 47-µm standard Millipore filtration assembly with Whatman® glass microfiber filters and connected to a D95 model DINKO vacuum pump (Dinko Instruments, Spain). Metal solutions were analysed by atomic spectroscopy using an iCE 3000 Series Atomic Absorption (AA) spectrometer (Thermo Scientific, USA) or an Iris Intrepid inductively coupled plasma atomic emission (ICP-AES) spectrometer (Thermo Elemental, USA). FTIR spectra were obtained using a Shimadzu IRAffinity-1S spectrophotometer (Shimadzu Corporation, Japan) using the PIKE MIRacle™ ATR sampling accessory (PIKE Technologies, USA). The morphology of biomass surface was determined by using the imaging capacity at the SEM-FEI Nova NanoSEM 450 with the secondary electrons detector (TLD-SE) (Nova, USA). The qualitative elemental analysis was also performed using the EDAX detector 100 mm^2 surface (AMETEK®, USA). A Nanotrac Wave dynamic light scattering (DLS) system (Microtrac, Germany) was used to measure the particle size and calculate the specific surface area.

2.2 Biosorbent preparation and characterisation

The Palomino Fino grape seeds were collected after vinification process. They were washed several times with deionised water, heated in oven at 40 °C until constant weight and cryogenically grinded. After that, the biosorbent was sieved through a 120-mesh size sieve (0.125 mm) with nylon mesh (CISA, Spain). This powder was stored in polyethylene bottles for further use.

2.2.1 Seed natural fats and oil extraction

The influence of the natural fats and oils on the sorption process was studied by comparison of the results obtained for defatted and non-defatted biomass. The Soxhlet method was performed to extract the fats from the biomass using 6 g of dried seed powder and 130 mL of n-hexane as solvent, keeping the reflux for 9 h [25].

2.2.2 Bulk and particle density

Density measurements were carried out using a 10-mL volumetric flask of known weight. Bulk density was carried out following the procedure described by Pholosi et al. [26]. The volumetric flask was filled with the biomass to the mark with gentle tapping to ensure the particles settle and remove all air spaces, and the bulk density was obtained as the mass of biomass occupying 10 mL. The apparent density (particle density) was evaluated by the measurement of the mass of particles divided by the volume of displaced water. For that, the flask was filled with 1 g of biomass and deionised water to the mark and weighed. It was also weighed containing only deionised water. The bulk volume occupied by the biomass was determined by comparing both mass values [27]. The porosity was also obtained by density measurements as described by Karim et al. [27] and the specific surface area was calculated by using DLS measurements.

2.2.3 Iodine adsorption capacity

The iodine adsorption capacity was carried out following the procedure described by Pholosi et al. [26]. A total of 50 mL of 0.005 mol L^{-1} I_2 solution was added to a flask containing 0.02 g of biosorbent and the suspension was stirred at 300 rpm for 24 h at 23 °C. The sample was filtered and 10-mL aliquots of the supernatant were titrated with 0.005 mol L^{-1} $Na_2S_2O_3$ using 1 mL of 1% starch solution as indicator. The iodine adsorption capacity was determined as the amount of iodine adsorbed per gramme of sorbent at the residual iodine concentration (mg I_2 g^{-1}).

2.2.4 FTIR spectroscopy

Structural analysis of biosorbent before and after the sorption process was performed by Fourier transform infrared spectroscopy (FTIR). The measurements were carried out in the region from 4000 to 600 cm^{-1} with a resolution of 4 cm^{-1} under attenuated total reflection (ATR) mode using an ATR sampling accessory.

2.2.5 SEM–EDX analysis

The surface morphology of the biomass was obtained by using a scanning electron microscope (SEM). The microscope was operated at accelerating voltage of 5 kV. The micrographs were taken with the sample previously deposited onto a carbon grid. The samples were coated by sputtering with a 15-nm gold layer to improve the conductivity in the analysis, obtaining a better image quality. Microanalysis was performed in an energy-dispersive X-ray spectrometer (EDXS).

2.2.6 Point of zero charge

The point of zero charge (pH_{pzc}) is the pH value at which the charge on the sorbent surface is zero. The pH_{pzc} value was assessed by the pH drift method (NaCl solutions) as follows: Aliquots of 50 mL of 2 mmol L^{-1} NaCl solutions were taken in different flasks and the initial pH values of each solution were adjusted in the range of 2–12 using 0.1 mol L^{-1} HCl or NaOH. Then, 0.2 g of biosorbent was added to each solution and their final pH values were measured after 24 h under shaking at 23 °C. The pH_{pzc} was determined from the pH_{final} vs. $pH_{initial}$ plot at the point where $pH_{initial} = pH_{final}$ [28].

2.2.7 Surface negative charge

The surface negative charge of the biosorbent was determined by a modification of the Boehm titration method [26, 29] which applies to acid sorbents. Acid groups are neutralised by sodium hydroxide, both strongly (e.g. carboxylic) and weakly (e.g. phenolic) groups. A total of 0.5 g of the biosorbent was kept in contact with 25 mL of 0.1 mol L^{-1} NaOH at 23 °C for 24 h and was shaken at 300 rpm. Subsequently, the solution was centrifuged and 10 mL of the supernatant was added to 15 mL of 0.1 mol L^{-1} HCl solution in an Erlenmeyer flask. The excess of HCl added in the solution prevented any possible adsorption of atmospheric carbon dioxide. Finally, the sample was titrated with 0.1 mol L^{-1} NaOH and the surface negative charge was expressed in mmoles H^+ per gramme of biosorbent.

2.3 Batch sorption studies

Batch experiments were performed by mixing 50 mL of 1 mmol L^{-1} metal solutions at pH 5.5 and 0.75 g of biosorbent into 100-mL polypropylene containers. The suspensions were stirred using an orbital laboratory shaker at 200 rpm for the set time (15–960 min) and temperature (18–30 °C). The resulting mixtures were filtered and the metal content in the aqueous solutions was analysed by AAS or ICP-MS according to the metal concentration. Experiments were performed in duplicate under the same conditions. The metal removal by the biosorption process (in percentage) was determined as follows:

$$Cr_{\text{biosorption}}(\%) = \frac{C_o - C_t}{C_o} x100 \tag{1}$$

where C_o and C_t are respectively the initial and t-time concentrations of Cr(VI) (mg L^{-1}) in the aqueous solution. The sorption capacity q_t (expressed in mg g^{-1}), defined as the amount of Cr(VI) sorbed per unit weight of biosorbent, was also calculated from the following equation:

$$q_t = \frac{(C_{0-}C_t) \cdot V}{m} \tag{2}$$

where V is the volume of the solution (L) and m is the mass of biosorbent (g). In addition, the equilibrium sorption capacity q_e (expressed in mg g^{-1}) was obtained as follows:

$$q_e = \frac{(C_{0-}C_e) \cdot V}{m} \tag{3}$$

where C_e is the equilibrium concentration of Cr(VI) (mg L^{-1}) in the aqueous solution (i.e. the unsorbed Cr(VI) concentration in solution at equilibrium).

2.4 Optimisation of the sorption process and data modelling

The optimisation of the sorption process was carried out by applying a 2^3 factorial design with two replicates of each experiment and four repetitions of the central point. The software *Statgraphics XVII* (Statpoint Technologies, Inc.,

USA) [30] was used for the statistical analyses. The data modelling to study the behaviour of chromium biosorption was processed on the MS Excel 2016 software (Microsoft Corporation, USA) with "user defined equations".

2.5 Sorption isotherm studies

The sorption isotherms were studied at 23 °C under the conditions mentioned in Sect. 2.3 by varying the initial concentration of Cr(VI) in the aqueous solution (0.25; 0.5; 1 and 1.5 mmol L^{-1}) at a fixed equilibrium time of 8 h. All experimental data were fit to linear forms of the Langmuir, Freundlich and Temkin isotherm models (Table 1) [31, 33].

2.6 Sorption kinetics studies

To study the sorption kinetic of Cr(VI) by the Palomino Fino grape seed biomass, experiments at 10 different periods of time (ranging from 15 to 960 min) with the same initial Cr(VI) concentration of 1 mmol L^{-1} in the aqueous solution were performed. The other conditions were keeping as mentioned in Sect. 2.3 and the temperature was controlled at 23 °C. Six different kinetic models were studied for their fit to the experimental data in order to understand the mechanism and rate-controlling step: pseudo-first order (Lagergren kinetic model) [34], pseudo-second order [34, 35], Elovich [36, 37], Ritchie's second order [38, 39], first-order reversible [34, 40] and intraparticle diffusion models [32, 34, 41]. The kinetics equations, their linear forms and the plots are summarised in Table 2 and the best-fitting kinetic model to the experimental data was evaluated by the determination coefficient (R^2).

2.7 Sorption thermodynamic studies

To study the effect of the temperature on the efficiency of Cr(VI) biosorption and determine the thermodynamic parameters of the process, batch experiments with an initial Cr(VI) concentration of 1 mmol L^{-1} in the aqueous solution were carried out at different temperatures (18, 23 and 30 °C) at a fixed equilibrium time of 8 h (the other conditions are described in Sect. 2.3).

Table 1 Sorption isotherm models evaluated in this study

Isotherm	Equation [a]	Linear form [a]	Plot
Langmuir [31]	$q_e = \frac{K_L q_{\max} C_e}{1+K_L C_e}$	$\frac{1}{q_e} = \frac{1}{q_{\max}} + \left[\frac{1}{K_L \cdot q_{\max}}\right] \cdot \frac{1}{C_e}$	$\frac{1}{q_e}$ vs. $\frac{1}{C_e}$
Freundlich [32]	$q_e = K_F C_e^{1/n}$	$\log q_e = \log K_F + \frac{1}{n} \log C_e$	$\log q_e$ vs. $\log C_e$
Temkin [33]	$q_e = \frac{RT}{b_T} \ln(K_T \cdot C_e)$	$q_e = B \ln K_T + B \ln C_e$ $B = \frac{RT}{b_T}$	q_e vs. $\ln C_e$

[a] K_L: Langmuir isotherm constant; $q_{\max}$: maximum adsorption capacity; K_F: Freundlich isotherm constant; n: measure of adsorption intensity; K_T: equilibrium binding constant; b_T: Temkin isotherm constant

Table 2 Theoretical kinetic models evaluated in this study

Model	Equation [a]	Linear form [a]	Plot
Pseudo-first order [34]	$\frac{\partial q}{\partial t} = k_1(q_e - q_t)$	$\log(q_e - q_t) = \log q_e - \left(\frac{k_1}{2303} t\right)$	$\log(q_e - q_t)$ vs. t
Pseudo-second order [34]	$\frac{\partial q}{\partial t} = k_2(q_e - q_t)^2$	$\frac{t}{q_t} = \left(\frac{1}{k_2 q_e^2}\right) + \frac{t}{q_e}$	$\frac{t}{q_t}$ vs. t
Elovich [36]	$\frac{\partial q}{\partial t} = \alpha e^{-\beta q_t}$	$q_t = \frac{1}{\beta} \ln \alpha\beta + \frac{1}{\beta} \ln t$	q_t vs. $\ln t$
Ritchie's second order [38]	$\frac{\partial(\theta)}{\partial t} = k_{2\_R}(1-\theta)^2$ $\theta = \frac{q_t}{q_e}$	$\frac{q_e}{q_e - q_t} = 1 + k_{2\_R} \cdot t$	$\frac{q_e}{q_e - q_t} - 1$ vs. t
First-order reversible [40]	$\frac{\partial q}{\partial t} = k_1(C_o - q_t) - k_2 q_t$	$\ln(1 - U_t) = -(k_1 + k_{-1})t$ $U_t = \frac{C_0 - C_t}{C_0 - C_e}$	$\ln(1 - U_t)$ vs. t
Intraparticle diffusion [32]	$q_t = K_d t^{\frac{1}{2}} + C$ derived from Fick's second law	$q_t = K_d t^{\frac{1}{2}} + C$	q_t vs. $t^{1/2}$

[a] k_1: rate constant of pseudo-first-order reaction; k_2: rate constant of pseudo-second-order reaction; α : initial adsorption rate in Elovich equation; β : desorption constant in Elovich equation; k_{2_R}: Ritchie's reaction rate constant; k_{-1}: rate constant of pseudo-first-order inverse reaction; K_d: intraparticle diffusion coefficient; C: intraparticle diffusion constant

3 Results and discussion

3.1 Biosorbent characterisation

3.1.1 Seed natural fats and oil extraction

The Soxhlet extraction showed an extraction yield of 21 wt% of fat content. The amount of Cr(VI) sorbed onto the Palomino Fino grape seed, before and after the fats and oil extraction, was evaluated and percentages of Cr(VI) biosorption were found to be 91.4 ± 0.3% and 85.1 ± 1.2%, respectively. These results indicated that the presence of fats and oils in the seeds could enhance the biosorption process. Therefore, further experiments were carried out using biomass not subjected to the Soxhlet extraction process.

3.1.2 Bulk and particle density

The bulk density (BD) is based on the space occupied by an amount of biomass particles and defined as the ratio of the mass of a powder sample and its volume, including the contribution of the inter-particulate void volume; for that, it depends on the way to pack the biomass. The apparent density (particle density) (AD) includes the internal pores of a biomass [26, 42]. The values obtained for the Palomino Fino grape seed biomass were 0.68 ± 0.05 g mL^{-1} for BD and 1.02 ± 0.09 g mL^{-1} for AD, with a 33.3% of porosity and a specific surface area of 15.2 ± 0.7 m^2 g^{-1}. Insoluble fibres found in grape seeds are characterised by high porosity and low density and these constituents are significant in this type of biomass [24]. The obtained density values were in the same range as other biosorbents used for metal removal from wastewater, usually from 0.25 to 3.5 g mL^{-1}. These slightly low values indicate a high contact surface, but are adequate for the filtration after sorption step; much lower density values would make filtration difficult. In fact, the lower limit of 0.25 g mL^{-1} for BD was set by the American Water Work Association [43] for granular activated carbon to be of practical use in filtration. Besides, values of apparent density close to the unity indicate higher contact between sorbate and sorbent [44]. Some examples of these values for BD are as follows: 0.33 and 0.55 g mL^{-1} for *Malacantha alnifolia* and *Pentaclethra macrophylla* tree bark biosorbents, respectively [45]; 0.73 g mL^{-1} for rice husk [46]; and 2 and 2.2 g mL^{-1} for black and green olive stones, respectively [47]. Other AD values are as follows: 1.17 g mL^{-1} almond tree (*Terminalia catappa L.*) leaves [44]; 1.5 g mL^{-1} for rice husk [46]; and 3 and 3.2 g mL^{-1} for black and green olive stones, respectively [47]. For these olive stones, the porosity values (31.3% and 33.3%, respectively) were similar than those obtained in this paper; however, their specific surface area values were lower (1.03 and 1.21 m^2 g^{-1}, respectively).

3.1.3 Iodine adsorption capacity

The iodine capacity (I, mg I_2 g^{-1}) is used to determine the adsorption capacity of a sorbent and as an approximation of the surface area (typical values range from 500 to 1200 mg g^{-1} and it is equivalent to a surface area between 900 and 1100 m^2 g^{-1} for activated carbon) [48]. It is defined as the mass of iodine (in mg) adsorbed per gramme of sorbent. This value is a measure of its porous structure and provides information about the ability to adsorb small and medium molecules (microporous: 0–2 nm; mesoporous: 2–50 nm) [49]. In addition, this parameter can be used to determine the degree of unsaturation in fatty acids where double bonds react with iodine compounds. The higher the iodine capacity, the more C=C bonds in the chemical structure of the biosorbent [50].

In the present work, the iodine capacity of the biomass was found to be 1600 ± 10 mg g^{-1}. This result is higher than typical values found in the literature, and even those obtained for activated biosorbents after an activation step by temperature treatment, such as, for instance, biochar obtained from pyrolysis of bamboo (*Dendrocalamus latiflorus* Munro) shoot shell (1254 mg g^{-1}) [51] and activated carbons prepared from seaweed *Sargassum longifolium* (1041 mg g^{-1}) and *Hypnea valentiae* (962 mg g^{-1}) [52]. In this paper, the insoluble fibre content of seeds [24] and the vinification process could improve the porous structure of the resulting Palomino Fino grape seed biomass yielding a high iodine adsorption; i.e. a high surface area and a largely microporous and mesoporous structure. Because of that, this biomass shows a great potential as sorbent with an easy and low-cost preparation.

3.1.4 FTIR analysis

The functional groups present in the biomass influence the biosorption process because they are responsible for metal ions binding. The 3 FTIR spectra of raw and defatted biomass and, also, Cr(VI)-loaded biomass after the biosorption process were used to identify functional groups and their possible changes (Fig. 1). The presence of numerous peaks in both region of functional groups (4000–1500 cm^{-1}) and fingerprint region (< 1500 cm^{-1}) indicated the heterogeneity and complex nature of the biomass; they are in line with the structural components of the grape seed and their predominant functional groups.

The broad band between 3600 and 3100 cm^{-1} showed by raw biomass is associated with the existence of –OH

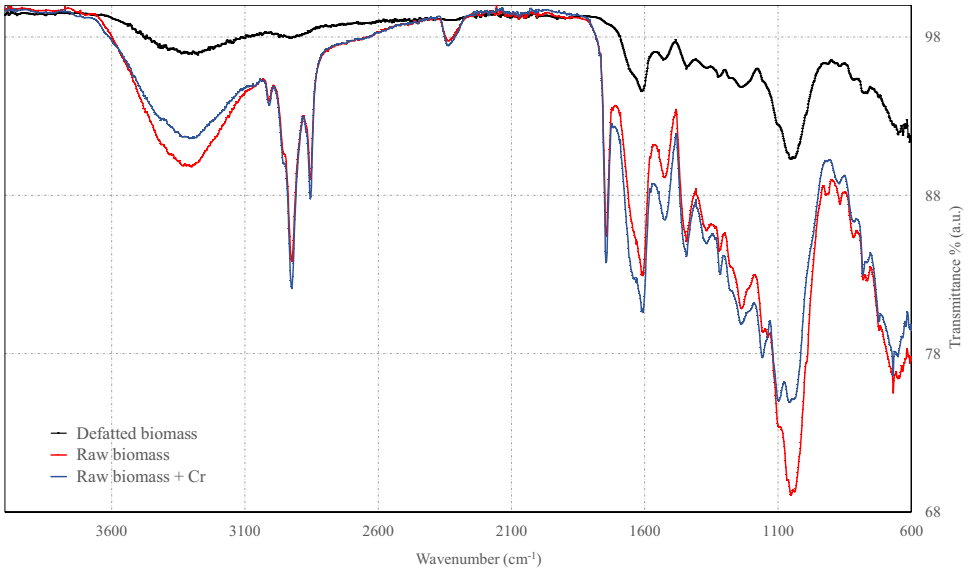

Fig. 1 FTIR spectra of Palomino Fino grape seed: (a) raw biomass; (b) defatted biomass; (c) Cr(VI)-loaded biomass after the biosorption process

and –NH stretching of hydroxyl and amine/amide groups of alcohols, phenols or carboxylic acids and to be able to develop hydrogen bonds. That is commonly associated with polysaccharides and lignins present in the seeds that provide rigidity to cellulose structures. The NH_2 group of proteins is another possible contribution. The C–H stretching vibration of the cis-double bond (=CH) groups was found at 3008 cm^{-1}, present in unsaturated fatty acid such as linoleic or oleic acids. Methyl (C–H), aliphatic methylene (CH_2) and methoxy ($–OCH_3$) stretching peaks were found at 2924 and 2854 cm^{-1} related to the methyl bonds and hydrophobic methylene/methoxy groups of hydrocarbon chains of lipids, lignin or tocopherols in grape seeds [23, 53, 54]. The peak found around 2330 cm^{-1} has been attributed to N–H or C=O stretching vibrations in grape bagasse [55]. Also, the peak at 1740 cm^{-1} corresponds to C=O stretching from ester groups as triglycerides. They are present in components of grape seeds such as fatty acids and their esters, pectin and lignin [54]. The band in the range of 1680–1600 cm^{-1} was associated with the stretching of C=C (aromatic ring), C=O (asymmetrical) in carboxyl group and N–H bending which can be found in phenolic compounds, pectin, hemicellulose or protein molecules [53, 55]. Phenolic compounds could rise the peaks at 1519 cm^{-1} and 1441 cm^{-1} associated with the aromatic C–C stretching, the peak at 1154 cm^{-1} from the C–H (aromatic) stretching and the peak at 781 cm^{-1} from the bending vibration of CH_2 (rocking). The peaks in the range of 1365–1232 cm^{-1} were assigned to the bending of CH_2 and O–H, and the stretching of C–O found in polysaccharides, and pectin. Other peaks from the fingerprint region were 1247 cm^{-1} and 1161 cm^{-1} that were associated with cyclic C–O–C groups, CH_3–CO–O– esters and C–H from aromatic compounds corresponding to lignocellulosic components of seeds. The absorption band of the –C–O stretching found in the range of 1098–1031 cm^{-1} was associated with polyphenols, phenols and other alcoholic groups (lignins, tannins, flavonoids…) or the phenyl bending in plane at 1085 cm^{-1} in tocopherols, being all of them present in a high percentage in grape seeds. Finally, the peaks found in the range from 920 to 800 cm^{-1} and 722 cm^{-1} are related to wagging of the $=CH_2$ or bending of the –HC=CH– (trans/cis) present in tocopherols and in unsaturated fatty acids.

These results found for grape seed biomass were in accordance with those reported by other authors for wine by-products [23, 53–57].

These results provided information about the functional groups that could be involved in the chromium biosorption. An increase of the carboxyl band (in the range of 1600–1680 cm^{-1}), associated with phenolic compounds (increase of 1519 cm^{-1} peak) and their aromatic C–C bonds (increase of 1154 cm^{-1} peak) as well as an increase of C=O from esters (increase of 1740 cm^{-1} peak), was obtained after chromium sorption. The new peak appearing at 1660 cm^{-1} is described in the literature for the reduction of Cr(VI) [58]. A significant decrease of the carbonyl band intensities (1098–1031 cm^{-1}) associated with polyphenols, phenols and other alcoholic groups was observed as well as a decrease in the broad band (3600–3100 cm^{-1}) of –OH groups. As suggested by the spectra, during the chromium biosorption, the C–O groups were oxidised into C=O and Cr(VI) was reduced to Cr(III) by those electron-donor groups. Thus, the changes of the spectra could be associated with the oxidising effect of the Cr(VI) and the coordination/ion exchange of the Cr(III) produced. The carboxyl groups in a moderately acid medium (around pH 5) behave as weak acids and make the interaction between the biomass and the Cr(III) cation easier [59].

The spectrum of the defatted biomass showed the extraction of these components from the grape seed biomass (Fig. 1, black line). The lack of fat content in the biomass yielded a lower biosorption percentage when used for the chromium sorption, providing evidence of their contribution to the process.

3.1.5 SEM–EDX analysis

The surface texture and morphological characteristic of the biomass before and after chromium sorption are shown in Fig. 2. The images clearly showed morphological differences due to the sorption process. The raw biomass surface was irregular with angular cuts and in form of flakes before the process. After the metal sorption, it appeared to be hazy, indicating the filling by the metal. The qualitative SEM–EDX analysis before (Fig. 3a) and after (Fig. 3b) sorption was performed and the elemental composition of the biomass was mainly found to be C, O, N, Ca, S, K, P, Cu and Mg where C and O result in ≈ 90%. The EDX spectrum of the raw and Cr(VI)-loaded biomass showed extra peaks of Cr(VI), confirming the biosorption phenomena.

3.2 Surface chemistry and behaviour of the biosorbent affected by the solution pH

The behaviour of the biosorbent in solution and the sorption process of Cr(VI) are highly affected by the pH, because the different chromium species in solution, the surface charge of the biosorbent and the ionisation degree of the functional

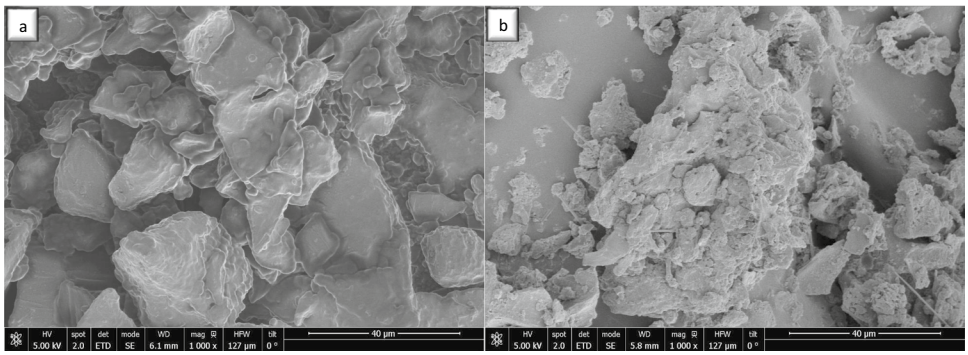

Fig. 2 SEM images of the Palomino Fino grape seed (at 1000 × magnification): (a) raw biomass; (b) Cr(VI)-loaded biomass after the biosorption process

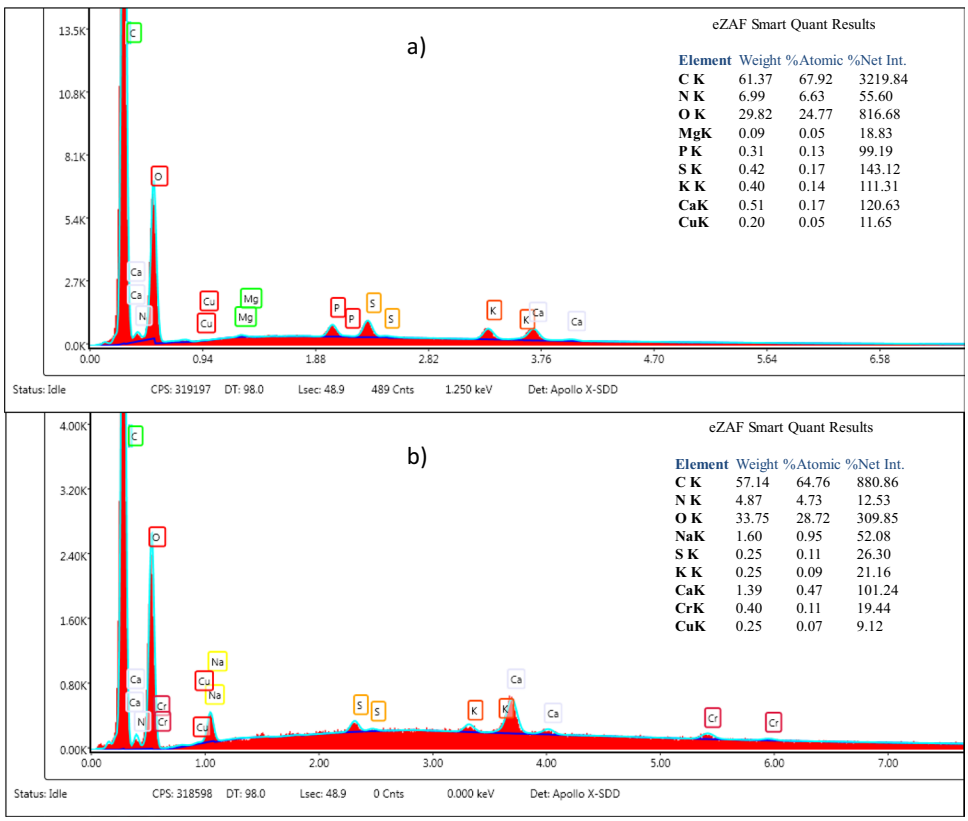

Fig. 3 EDX analysis of the Palomino Fino grape seed: (a) raw biomass; (b) Cr(VI)-loaded biomass after the biosorption process

groups depend on the acid/basic conditions (principally, -OH, -COOH, -NH_2) [60].

3.2.1 Speciation of Cr(VI)

In aqueous solution, Cr(VI) speciation depends on the pH and metal concentration. The equilibria at low Cr(VI) concentration (< 0.01 g L^{-1} (0.2 mM)) are as follows:

$$H_2CrO_4 + H_2O \rightleftharpoons HCrO_4^- + H_3O^+$$

$$HCrO_4^- + H_2O \rightleftharpoons CrO_4^{2-} + H_3O^+$$

where the pKa1 value is lower than 1.5 and the pKa2 ranges from 5.76 to 7 in the temperature range of 20–25 °C (according to the experimental conditions used in this paper). The predominant species are $HCrO_4^-$ at acid conditions (pH 0.75–6.45) and H_2CrO_4 at highly acid conditions (pH < 0.75) [61, 62]. When the concentration of Cr(VI) increases, the chromate/dichromate equilibrium occurs:

$$2HCrO_4^- \rightleftharpoons Cr_2O_7^{2-} + H_2O$$

Studies with higher concentrations of Cr(VI) showed a higher stability of $Cr_2O_7^{2-}$ which improved with higher ionic strength [63]. Thus, it is described that for 50 mM Cr(VI) in 3 M KCl, the predominant species is $Cr_2O_7^{2-}$ in acid medium (pH 0.75–6.45) and $HCr_2O_7^-$ at lower pH values [62]. By last, CrO_4^{2-} is the predominant species at neutral to basic pH regardless of the concentration.

In this work, previous batch experiments at different pH values were performed to know the acid conditions for the sorption of Cr(VI), obtaining the following percentages of removal: 67.4% at pH 3; 87.4% at pH 4.8; and 54.7% at pH 6 with 1 mM of metal and 10 mg L^{-1} of biosorbent. In these conditions, $HCrO_4^-$ and $Cr_2O_7^{2-}$ species were in equilibrium in the solution.

3.2.2 Point of zero charge

Related to the surface charge, the point of zero charge pH_{pzc} is defined as the pH at which the surface charge of the sorbent is zero. It depends on the chemical and electronic properties of the functional groups on its surface and gives information about the affinity of the biomass for cationic or anionic species depending on the pH of the solution. Its quantification is an input to understand the mechanism of the sorption process under varying pH conditions. The surface charge of the biomass is positive at $pH < pH_{pzc}$ and negative at $pH > pH_{pzc}$. Thus, the sorption of metal ions can be enhanced when $pH > pH_{pzc}$, particularly for those that exist in cationic form and, conversely, when $pH < pH_{pzc}$ for those present in anion form. This can suggest a significant presence of electrostatic forces in the adsorption process [10]. The pH_{pzc} was found to be 5.2 for Palomino Fino grape seed biomass. It is expected that sorption experiments at pH values close to this value take place without electrostatic repulsion for anionic Cr species, such as those carried out in this work.

3.2.3 Surface negative charge

The surface negative charge can be associated with the ionisation of acidic functional groups on the biomass surface. These acidic groups, both strongly (e.g. carboxylic) and weakly (e.g. phenolic), provide potential surface adsorptive sites for the biosorption of metal ions [29]. The surface negative charge value for Palomino Fino grape seed was 2.4 ± 0.2 mmol g^{-1}. This result shows a higher surface negative charge if compared with other grape sorbents, such as different grape bagasse chars (0.12–0.27 mmol g^{-1}) used for Hg(II) sorption [57], grape stalk wastes (1.20–1.73 mmol g^{-1}) used for some cations (Cd(II), Pb(II), Hg(II)…) [64] or grape waste-derived nanoporous carbon (1.25 mmol g^{-1}) used for Cu(II) sorption [82]; it was also higher if compared with some biomass used for Cr(VI) sorption: durian shell (Monthong variety) (0.514 mmol g^{-1}) [65], orange peel [66] or wheat bran (0.43 mmol g^{-1}) [67]. Thus, the grape seed showed promising potential as biosorbent.

3.3 Optimisation of the sorption process

The optimisation of the Cr(VI) removal by sorption was carried out using a 2^3 (two-level) factorial design for the following factors: pH value of the solution, amount of biosorbent and contact time. Twenty experiments including two replicates of each experiment and four repetitions of the central point were performed. The levels for the factors were selected based on the previous experiments abovementioned and encoded as upper level (+ 1), central point (0) and lower level (− 1), as shown in Table 3. The central point was used to check the linear response of the variables to be used in the two-level factorial design. The experiments were carried out using 1 mmol L^{-1} of Cr(VI) solutions buffered with 0.1 mol L^{-1} CH_3COOH-CH_3COONa at 23 °C.

Table 3 Factor levels and selected values used in the 2^3 experimental design with central point

Variable	Lower level (− 1)	Central point (0)	Upper level (+ 1)
pH	3.5	4.5	5.5
Biosorbent (g L^{-1})	5	10	15
Time (h)	8	16	24

Table 4 Matrix of the 2^3 experimental design (two replicates of each experiment and four repetitions of the central point) and the experimental response for the Cr(VI) biosorption

Experiment	pH	Biosorbent ($g\ L^{-1}$)	Time (h)	$Cr(VI)_{biosorption}$ (%)
1	5.5	15	24	93.5
2	5.5	15	8	92.1
3	3.5	15	8	76.7
4	3.5	15	24	73.4
5	4.5	10	16	82.5
6	5.5	5	8	87.7
7	3.5	5	8	79.6
8	5.5	5	24	89.7
9	3.5	5	24	75.3
10	4.5	10	16	83.0
11	5.5	15	24	93.5
12	5.5	15	8	92.6
13	3.5	15	8	76.9
14	3.5	15	24	73.0
15	4.5	10	16	83.5
16	5.5	5	8	87.8
17	3.5	5	8	80.1
18	5.5	5	24	89.9
19	3.5	5	24	76.1
20	4.5	10	16	83.6

The matrix of the variables for the factorial design and the experimental results are shown in Table 4.

Once the linear relationship between the independent variables and the response was checked, the experimental data were analysed. According to the Pareto chart (Fig. 4), the pH showed a significant positive effect on the percentage of Cr(VI) biosorption at a confidence level of 95%, being 5.5 the optimum level (+1). Higher values of this upper level yielded lower removal of chromium as above-mentioned. The contact time showed a non-significant negative effect, while the amount of biosorbent showed a non-significant positive effect. The relationships between the response and the independent variables were also analysed by means of the response surface and contour plots of the interactions (Fig. 5). Hence, the optimal removal of Cr(VI) was achieved at pH 5.5 and for further experiments 15 g L^{-1} of biosorbent (level: +1) and 8 h of contact time (level: −1) were also selected as suggested by the experimental design analysis.

To verify if the selected time was enough to reach the equilibrium state of the sorption process, several Cr(VI) solutions in the range of 0.25–1.5 mmol L^{-1} were studied. The experimental data showed that the equilibrium was reached after 8 h for all the concentrations studied (Fig. 6) as suggested by the optimisation of the sorption process. The uptake rate was initially very rapid, with > 85% of metal biosorption at 2 h (120 min) and close to those percentages obtained until reaching the equilibrium state.

3.4 Analytical features of the biosorption process

Under the optimal conditions, the precision of the method was determined by six replicate biosorption experiments using 1 mmol L^{-1} of Cr(VI) at 23 °C. The average of metal removal in percentage ($Cr_{biosorption}$ (%)) was 91.7 ± 0.6, being the precision of the method of 0.64% at a confidence level of 95%. The effect of Cr(VI) concentration on the equilibrium sorption capacity (q_e) was also investigated in a range from 0 to 2 mmol L^{-1} with three replicates for each standard solution. It was calculated by Eq. (3) but expressed as Cr(VI) mmol g^{-1}. As shown in Fig. 7, the equilibrium sorption capacity linearly increased along with the concentration of Cr(VI), being the equation of the linear regression as:

$$q_e\left(mmol g^{-1}\right) = \left(0.0587 \pm 1.67 \cdot 10^{-4}\right) \cdot [Cr(VI)]\left(mmol L^{-1}\right) + \left(2.64 \cdot 10^{-4} \pm 1.72 \cdot 10^{-4}\right) \quad (4)$$

with a very remarkable determination coefficient ($R^2 = 0.9999$).

3.5 Sorption isotherms

The study of isotherms in the sorption process is a very useful tool used in predicting the maximum sorption capacity of the biosorbent [68], i.e. to characterise the adsorption equilibrium relationship at a fixed temperature between the

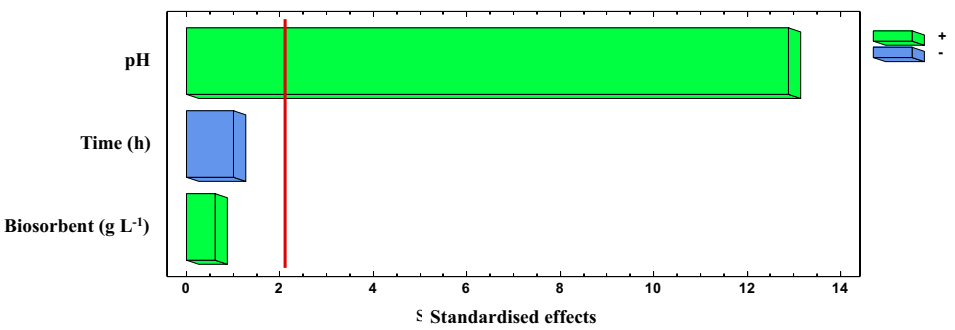

Fig. 4 Pareto chart for 2^3 experimental design (*red line*: significance level of 5%)

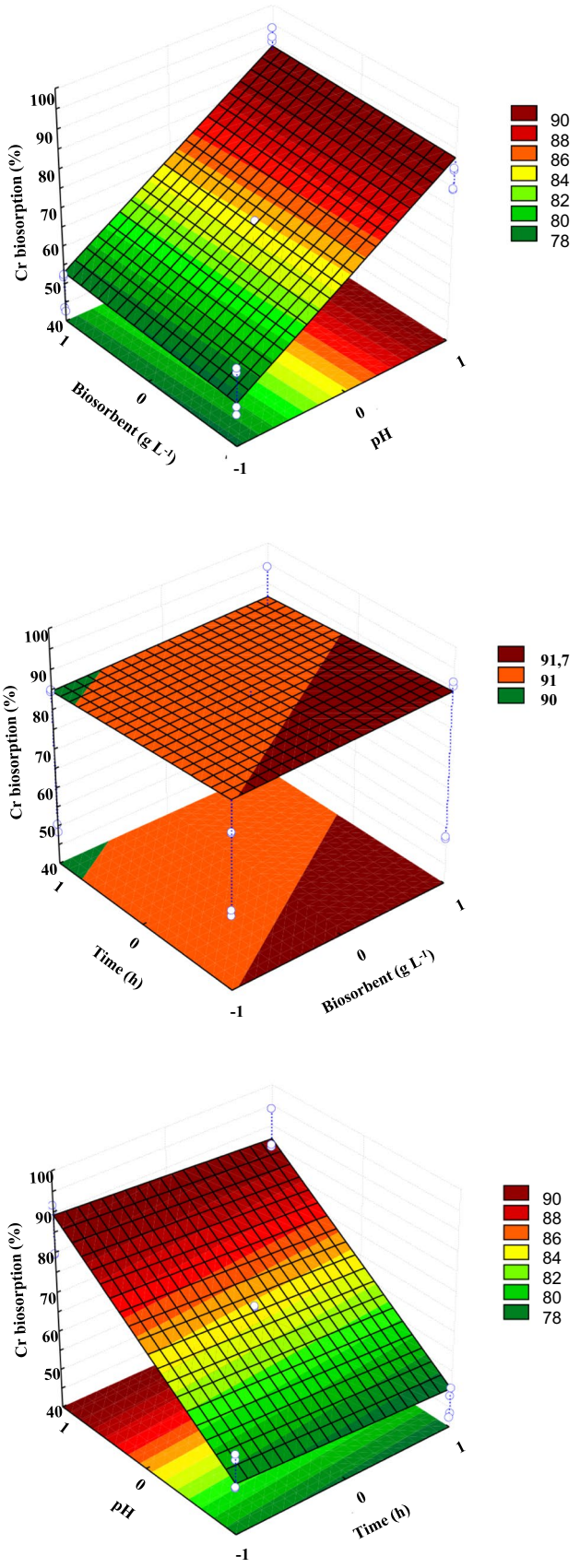

Fig. 5 Response surface and contour plots of factor interactions on the Cr(VI) biosorption percentage: (a) biosorbent amount—pH value interaction (factor level for contact time: [− 1]); (b) biosorbent amount—contact time interaction (factor level for pH: [+ 1]); and (c) contact time—pH value interaction (factor level for biosorbent amount: [+ 1])

metal ion (sorbate) concentration retained on the biomass (i.e. the equilibrium sorption capacity q_e) and in solution (i.e. the equilibrium concentration of metal ion in the aqueous solution C_e); this relationship predicts how the interaction occurs under the operating conditions. Different models can be used to fit the experimental data, being Langmuir, Freundlich and Temkin isotherms the most commonly used. The empirical equations, the linear forms and the plotted parameters used to fit the experimental data in this paper are detailed in Table 1.

The Langmuir isotherm considers that the sorption process occurs with the following: (a) formation of a monolayer on the biosorbent surface of; (b) no interaction between molecules adsorbed on neighbouring locations; and (c) all the sites are identical and energetically equivalent [31, 33, 68]. The chemisorption is usually explained as this single-layer process. K_L (L mg^{-1}) is the Langmuir isotherm constant and provides the affinity of the metal ion for the binding sites. The maximum value of the sorption capacity q_{max} (mg g^{-1}) is predicted by the model and it would be obtained in fully covered surface as monolayer. Another parameter can be obtained from the Langmuir isotherm using the following equation:

$$R_L = \frac{1}{1 + K_L \cdot C_o} \tag{5}$$

where R_L (separation factor) estimates the degree of suitability. The range of this dimensionless factor can be defined as unfavourable ($R_L > 1$), linear ($R_L = 1$), favourable ($0 < R_L < 1$) and irreversible ($R_L = 0$) [33].

The Freundlich isotherm describes the process as a multilayer sorption onto a heterogeneous surface and allows interaction between the biosorbent molecules [68]. This model proposes that active binding sites with different energy on the biosorbent exist and that those with higher binding strength will be firstly occupied by the metal ions; also, the binding strength of each site will decrease throughout the biosorption process [69]. The forming multiple layers are usually associated with physical sorption. K_F (mg g^{-1}) is the Freundlich isotherm constant related to the heterogeneity of the biomass surface and its activity as sorbent, the parameter n (g L^{-1}) is a measure of the nature and intensity of the biosorption process and its inverse value $1/n$ (L g^{-1}) is known as the heterogeneity factor. This model assumes

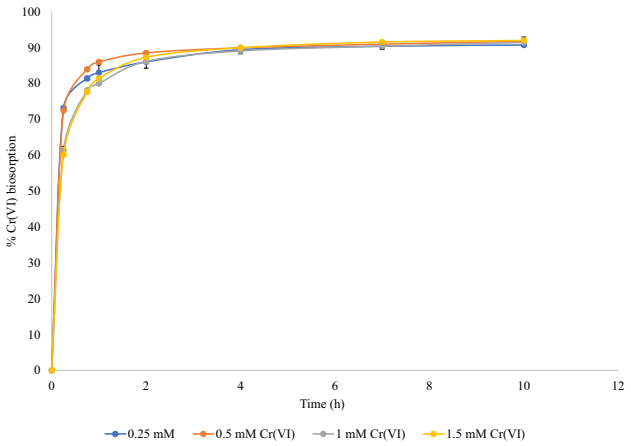

Fig. 6 Effect of contact time on the biosorption percentage of Cr(VI) onto Palomino Fino grape seed for Cr(VI) initial concentration in the range of 0.25–1.5 mmol L^{-1}

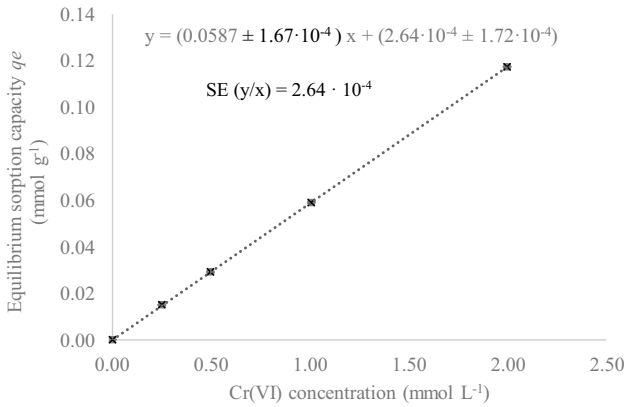

Fig. 7 Effect of Cr(VI) concentration on the equilibrium sorption capacity q_e (mmol g^{-1}) of the Palomino Fino grape seed

that if n is equal to 1, then the linear biosorption occurs and leads to identical adsorption energies for all binding sites; the biosorption is a chemical process for $n < 1$ and a physical process for $n > 1$ [70].

The Temkin model is based on the assumption that heat of biosorption of monolayer varies linearly with the temperature [33, 68]. This model suits well for gas phase equilibria but it usually fails to explain the equilibria of heavy metal in solid–liquid phase because the biomass molecules do not organise themselves in a similar packed structure. K_T (L mg^{-1}) is the equilibrium binding constant, related to the maximum binding energy; the B constant can be expressed with the equation $B = RT/b_T$ as function of the R constant (universal gas constant, 8.314 J mol^{-1} K^{-1}), the temperature T (K) and the Temkin isotherm constant b_T (J mol^{-1}), and it is related to the adsorption heat.

Constants and determination coefficients of the three models, determined from the fit of the linear plot at 23 °C, are listed in Table 5. The comparison of the predicted values by the fits of the three isotherm models and the experimental data is shown in Fig. 8 where the equilibrium data were plotted as q_e vs. C_e at 23 °C. The determination coefficients of the fits for the Langmuir and Freundlich models were high and similar. Therefore, a chemical or physical biosorption of Cr(VI) by the Palomino Fino grape seed could be explained by each fit, respectively. However, it is described that these mechanisms may sometimes occur on the biomass surface at the same time. In addition, the plots of the linearised isotherms (Fig. 8) showed that the Freundlich isotherm leaded to a better fit with the experimental data. The fit of Temkin isotherm was worse ($R^2 = 0.892$).

The maximum sorption capacity q_{max} for Cr(VI) was 208.3 mg g^{-1} (Table 5), being a higher value than the common values for different biosorbents found in the literature (e.g. a review of pollutant removal using agricultural waste describes q_{max} values ranging from 3.51 to 90.90 mg Cr(VI) per gramme of biomass [11]). In the same sense, the review of Redha [7] compares the q_{max} of several biosorbents where only non-living *Cupressus lusitanica* bark showed a higher q_{max} of 305.4 mg Cr(VI) per gramme. The affinity of the biomass for the Cr(VI) defined by K_L was 0.003 L mg^{-1}, which is a low value if compared with other biosorbents, such as Teff straw (0.33 L mg^{-1}) with chemisorption mechanism [71]; casuarinas fruit powder (0.097 L mg^{-1}) or sorghum stem powder (0.055 L mg^{-1}) with electrostatic sorption [72]; although similar values were found in other studies for rice husk (0.002 L mg^{-1}) with metal reduction and ion exchange mechanism [73]; or bone char (0.0023 L mg^{-1}) with a good suitability for Langmuir model and a chemisorption mechanism by generating new chemical species on the bone char surface [74]. The R_L values for grape seed were also calculated and ranged from 0.768 to 0.961, meaning the favourable sorption process for the chromium concentrations studied and feasible onto the Palomino Fino grape seed biomass.

The Freundlich isotherm defines the sorption of the Cr(VI) by the grape seed biomass as heterogeneous and the n value of 0.94 g L^{-1}, very close to 1, led to an increase in the concentrations of biosorbed Cr(VI) as its concentration increases in the aqueous solution (linear biosorption) (Fig. 7). The value of K_F was 0.593 mg g^{-1}. A comparison with the above-mentioned sorbents shows that the K_F value was similar than those obtained by Teff straw (0.798 mg g^{-1}), lower than those obtained by casuarinas fruit powder (1.845 mg g^{-1}), sorghum stem powder (1.704 mg g^{-1}) or rice husk (1.704 mg g^{-1}); and higher than those obtained by bone char (0.138 mg g^{-1}) [71–74].

Table 5 Isotherm constants and determination coefficients for Cr(VI) sorption onto Palomino Fino grape seed biosorbent

Isotherm models	Isotherm constants and determination coefficients [a]
Langmuir	$K_L = 0.003$ L mg^{-1} (0.156 L mmol^{-1}) $q_{max} = 208.3$ mg g^{-1} (4.01 mmol g^{-1}) $MSE = 0.0414$ $R^2 = 0.993$
Freundlich	$K_F = 0.593$ mg g^{-1} ($1.14 \cdot 10^{-2}$ mmol g^{-1}) $n = 0.94$ g L^{-1} $MSE = 0.0331$ $R^2 = 0.991$
Temkin	$B = 2.48$ $K_T = 0.916$ L mg^{-1} (47.61 L mmol^{-1}) $B = 989.4$ J mol^{-1} $MSE = 0.6637$ $R^2 = 0.892$

[a] *MSE*: mean square error

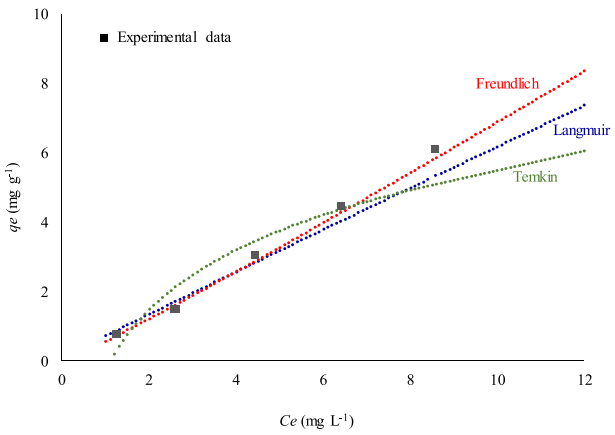

Fig. 8 Comparison of the predicted values by the fits of the isotherm models and the experimental data

3.6 Sorption kinetics

The kinetics of the sorption process provides valuable information to identify the possible mechanism and the rate-controlling step.

The models of sorption kinetics are applied in the rate determination of the metal removal. The kinetics of the process provides useful information to identify the possible mechanism which depends on the physical–chemical property of the sorbent and mass transport process [75]. Several kinetic models (Table 2) were studied by the fit of the experimental data for the removal of Cr(VI) onto Palomino Fino grape seed. The kinetic parameters were calculated from the plots (Table 6) and the coefficient of determination R^2 was used to test the best-fitting kinetic model to the experimental data.

The pseudo-first-order model proposes that the sorption rate at the binding sites is proportional to the number of unoccupied sites in the biomass, being a physical mechanism. The pseudo-second-order kinetic model associates the biosorption capacity with the available sites on the biomass surface where chemical reactions (exchange of electrons or by sharing of valence forces between the sorbent functional groups and metal ions) are involved [76]. The Ritchie's model is also a second-order kinetic model that considers that the adsorption rate depends only on the fraction of free active sites. The Elovich model considers the heterogeneity of the biomass surface. The first-order reversible model considers that the rate of the adsorption reaction (k_1) and the desorption rate (k_{-1}) constants are equal to the equilibrium reaction rate constant. The intra-particular diffusion model (derived from Fick's second law of diffusion) assumes that intraparticle diffusion is the rate-controlling step in the sorption process [3, 32, 69].

The pseudo-second-order model was the best model describing the sorption of Cr(VI) onto the proposed biomass with $R^2 = 1$, although the pseudo-first-order model also fits with a good coefficient ($R^2 = 0.983$). These results led that chemical interactions occurred between the Cr(VI) and the biomass as the pseudo-second order proposed, but the physical sorption interactions were also present by the good fit of the pseudo-first order. Also, the Elovich model showed a fit with a good R^2 value of 0.931, describing the chemisorption produced on an energetically heterogeneous surface of the biomass as Freundlich showed in the above isotherm study. The reversible model is usually valid for physical sorption but the value of $R^2 < 0$ obtained showed that other mechanisms could be involved in the chromium removal. The diffusion step in the biomass particles was not significant because of the low fit of the intraparticle model.

3.7 Sorption thermodynamic studies

Thermodynamic studies are applied to investigate the nature on the biosorption process. The standard Gibbs free energy (ΔG^o), the standard enthalpy change (ΔH^o), the standard entropy change (ΔS^o), the activation energy (E_a) and the sticking probability (S^*) are thermodynamic parameters that can be obtained by the following equations [77]:

$$\Delta G^o = -RT \cdot \mathrm{Ln} K_c \tag{6}$$

$$\Delta G^o = \Delta H^o - T \cdot \Delta S^o \tag{7}$$

$$S^* = (1 - \theta) \cdot e^{-\frac{E_a}{RT}} \tag{8}$$

The combination of Eqs. (6) and (7) and its subsequent linearisation allows to obtain this equation:

Table 6 Sorption rate constants and determination coefficients associated with the kinetic models for Cr(VI) sorption onto Palomino Fino grape seed biosorbent

Kinetic models	Kinetic parameters and determination coefficients [a]	
	1 mM Cr(VI)	1.5 mM Cr(VI)
Pseudo-first order	$k_1 = 0.0100$ min^{-1} $MSE = 0.0094$ $R^2 = 0.983$	$k_1 = 0.0099$ min^{-1} $MSE = 0.0153$ $R^2 = 0.973$
Pseudo-second order	$k_2 = 0.031$ g mg^{-1} min^{-1} $MSE = 0.0643$ $R^2 = 1$	$k_2 = 0.025$ g mg^{-1} min^{-1} $MSE = 0.093$ $R^2 = 1$
Elovich	α=48.44 mg g^{-1} min^{-1} β=3.458 g mg^{-1} $MSE = 0.0121$ $R^2 = 0.931$	$\alpha = 160.9$ mg g^{-1} min^{-1} $\beta = 2.593$ g mg^{-1} $MSE = 0.0029$ $R^2 = 0.906$
Ritchie's second order	$k_{2\_R} = 0.376$ min^{-1} $MSE = 1096.6$ $R^2 = 0.814$	$k_{2\_R} = 0.456$ min^{-1} $MSE = 2283.9$ $R^2 = 0.760$
First-order reversible	$k_1 = 0.011$ min^{-1} $k_{-1} = 0.001$ min^{-1} $MSE = 1.499$ $R^2 < 0$	$k_1 = 0.013$ min^{-1} $k_{-1} = 0.001$ min^{-1} $MSE = 1.291$ $R^2 = 0.355$
Intraparticle diffusion	$K_d = 0.048$ mg g^{-1} min$^{-1/2}$ $C = 2.25$ mg g^{-1} $MSE = 0.0393$ $R^2 = 0.775$	$K_d = 0.063$ mg g^{-1} min$^{-1/2}$ $C = 3.36$ mg g^{-1} $MSE = 0.083$ $R^2 = 0.739$

[a] *MSE*: mean square error

$$\mathrm{Ln}K_c = \left(\frac{\Delta S^\circ}{R}\right) - \left(\frac{\Delta H^\circ}{R}\right) \cdot \frac{1}{T} \tag{9}$$

where K_c is the equilibrium constant (L g^{-1}), R is the universal gas constant (8.314 J mol^{-1} K^{-1}), T is the temperature (K) and θ is the surface coverage. The parameters θ and K_c are defined by the following equations:

$$\theta = 1 - \frac{C_e}{C_0} \tag{10}$$

$$K_c = \frac{q_e}{C_e} \tag{11}$$

Therefore, enthalpy and entropy variation values were calculated from Eq. (9) using the plot of $Ln\ K_c$ vs. $1/T$, where the terms $(-\Delta H^\circ/R)$ and $(\Delta S^\circ/R)$ are the slope and the intercept of the fit. From the modified Arrhenius equation, described as Eq. (8) and its subsequent linearisation, the parameters E_a and S^* were determined. Thus, the plot of Ln (1-θ) vs. $1/T$ allowed the calculation of E_a/R as the slope of the curve and Ln S^* as the intercept.

The results for the enthalpy (ΔH°) and entropy (ΔS°) changes of the chromium sorption were 8.63 kJ mol^{-1} and 0.049 kJ mol^{-1} K^{-1}, respectively. The positive value of ΔH° indicated the process as endothermic. If this parameter is lower than 4.2 kJ mol^{-1} (1 kcal mol^{-1}), the predominant mechanism for sorption is physisorption with weak forces while the prevalence of chemical sorption shows higher sorption heat (21–420 kJ mol^{-1}). The intermediate value of ΔH° obtained could indicate a possible combination of physical and chemical mechanisms as suggested by the kinetic studies. The positive value of ΔS° associated with an increase in randomness at the solid–liquid interface suggested an ion exchange process and the affinity of the biomass towards chromium ions [78]. The values of standard Gibbs free energy were found to be − 5.59, − 5.83 and − 6.18 kJ mol^{-1} at 18 °C, 23 °C and 30 °C, respectively, which indicated the spontaneous nature of the chromium removal. Also, these values increased with temperature, promoting the sorption.

The positive value of E_a (5.34 kJ mol^{-1}) was consistent with the positive value of ΔH° and the endothermic nature of the adsorption process. The parameter S^* is a measure of the potential of the biomass to retain the sorbate. Values of S^* ranging in the interval of $0 < S^* < 1$ indicate a favourable sticking with a relevant physisorption mechanism. If S^* is equal to 0, then the predominant mechanism is chemical with an indefinite sorption of the sorbate. The obtained S^* value in this paper was 0.01, being able to explain a behaviour practically at the frontier of both mechanisms [79].

3.8 The mechanisms of the biosorption

Biosorption involves different mechanisms such as complexation/chelation, ion exchange, electrostatic attraction, covalent forces, van der Waals forces, surface adsorption and even precipitation or crystallisation. Sometimes, more

than one mechanism may take place and the biosorption can be a mechanistically complex process [3, 8].

That is the case of the removal of Cr (VI) by biomass. The most frequently proposed mechanism considers the sorption mechanism where anionic Cr(VI) species bind to the positive surface of biomass in acid conditions by electrostatic attraction [80]. Cr (VI) may remain in the hexavalent state in presence of small amount of electron-donor groups. However, in the presence of adequate amount of adjacent-reducing groups, it is considered that the low pH values can promote the reduction reaction, since the protons participate in the reaction [81]. After that, Cr(III) can be released to the solution by the electrostatic repulsion from the positive surface or complexed by functional groups (such as carboxyl or phenolic groups) of the biomass [58]. Other proposals covering a most wide pH range consider the adsorption mechanism by electrostatic interaction (by van der Waals forces: physical adsorption), ion exchange or surface complex formation before the reduction step may or may not take place [7]. As alternative to these mechanisms, a direct reduction of Cr(VI) in solution by contact with electron-donor groups of biomass is also proposed [80, 82], after which the Cr(III) is retained by the biomass wherein the mechanisms involved may be ion exchange, complexation or electrostatic attraction at $pH > pH_{pzc}$. It should be noted that the sorption of the produced Cr(III) usually decreases at $pH > 6.0$ because chromium hydroxides are produced [8, 59].

In this paper, the proposed mechanism for Palomino Fino grape seed biomass can be explained as a physical sorption coupled with a reduction reaction. This model is based on the optimal pH of the process ($pH = 5.5$), the characteristics of the biomass and the kinetic, equilibrium and thermodynamic studies, as a combination of a physical and chemical mechanisms. Cr(VI) interacts with the biomass by physical sorption as explained by the good fit of Freundlich isotherm and a low chemical affinity for the anionic chromium because the surface of the biomass is slightly negatively charged at the pH of process. As the sorption pH was very close to the pH_{pzc}, the anionic Cr(VI) species presented in the diffusion layer were principally retained through physical forces but not by electrostatic attraction.

Subsequently, they can be easily reduced to Cr(III) by the electron-donor groups of the biomass, mainly the tannins and phenolic groups present within the grape seed. The Cr(III), that exists as the main ion at the sorption pH, as above-mentioned, may be predominantly retained by the biomass through a chemical process, either by complexation with functional groups or by ion exchange (carboxylic compounds), providing enough stability to the chromium removal and a high maximum sorption capacity ($q_{max} = 208.3$ mg g^{-1}). Higher Cr(VI) concentrations enhance the reduction reaction and the biosorption is linearly promoted as indicated by n value of the isotherm [53]. This successful biosorption is based on the special grape seed components with a relevant content in antioxidant and lignocellulosic compounds (e.g. lignins, polyphenols, tocopherols, tannins).

It is worth noting that few sorbents are found in the literature that remove Cr (VI) at slightly acidic or neutral pH. Also, they require the addition or modification of the biomass to include reducing agents (as humic acid [83] or the use of reducing living organisms (as *Escherichia coli* [84] or *Pseudomonas alcaliphila* NEWG-2 [85]) to perform the sorption. Therefore, the proposed biomass provides two important eco-friendly advantages: The sorption process occurs at a slightly acidic pH (less hazardous) and the biomass can be used directly without chemical modification or addition of any reducing agent. In addition, the pH conditions close to neutral values (pH 6) are frequently found in the literature and reported as optimal values for the sorption of cationic metals in solutions [6], but not for Cr(VI). That is another drawback if simultaneous removal of metallic species wants to be approached. This drawback can be overcome by using the proposed biomass.

In this regard and as future perspectives, the simultaneous removal with other metals can be exploited given the promising results from some previous experiments carried out at slightly acid or close neutral pH values with Pb(II) (86%), Cd(II) (33%) or Co(II) (33%).

4 Conclusion

In this paper, a Sherry wine industry by-product, Palomino Fino grape seed, is proposed as biosorbent for the removal of Cr(VI) from aqueous medium obtaining satisfactory results. The biomass was characterised by means of several studies and the sorption process was optimised. Best experimental results were observed at slightly acidic pH without modification of the biomass or the addition of any reducing agent and it is based on the special grape seed composition. Also, sorption thermodynamic studies revealed that the nature of the biosorption is found to be spontaneous and endothermic and it can be explained as the combination of a physical and chemical sorption mechanism. The pseudo-second-order kinetic model is the best describing the sorption of Cr(VI) onto the proposed biomass, although the pseudo-first-order model also fits the experimental data quite well, explaining the chemical interactions between Cr(VI) and the biomass as well as the physical sorption.

This locally available and low-cost industrial by-product presents an easy preparation as a biosorbent and its potential use for the removal of Cr(VI) and other heavy metal ions shows interesting advantages to be applied.

Acknowledgements The authors wish to thank technician A. Olachea Arce for the supply of samples. Thanks are also due to Prof. A. Gil Montero for FTIR analysis.

Funding Open Access funding provided thanks to the CRUE-CSIC agreement with Springer Nature. This work has been supported by "Consejería de Economía, Conocimiento, Empresas y Universidad", Andalusian Government (Spain) (support for RNM-236 Research group) and the Programme of "Fomento e Impulso de la Investigación y de la Transferencia" from the University of Cadiz (Spain) (Project PR2020-013).

References

1. Kumar V, Parihar RD, Sharma A, Bakshi P, Sidhu GPS, Bali AS, Karaouzas I, Bhardwaj R, Thukral AK, Gyasi-Agyei Y, Rodrigo-Comino J (2019) Global evaluation of heavy metal content in surface water bodies: a meta-analysis using heavy metal pollution indices and multivariate statistical analyses. Chemosphere 236:124364. https://doi.org/10.1016/j.chemosphere.2019.124364
2. Vareda JP, Valente AJM, Durães L (2019) Assessment of heavy metal pollution from anthropogenic activities and remediation strategies: a review. J Environ Manage 246:101–118. https://doi.org/10.1016/j.jenvman.2019.05.126
3. Beni AA, Esmaeili A (2020) Biosorption, an efficient method for removing heavy metals from industrial effluents: a review. Environ Technol Innov 17:100503. https://doi.org/10.1016/j.eti.2019.100503
4. Ahmaruzzaman M (2011) Industrial wastes as low-cost potential adsorbents for the treatment of wastewater laden with heavy metals. Adv Coll Interface Sci 166(1–2):36–59. https://doi.org/10.1016/j.cis.2011.04.005
5. Ibrahim WM, Hassan AF, Azab YA (2016) Biosorption of toxic heavy metals from aqueous solution by *Ulva lactuca* activated carbon. Egyptian Journal of Basic and Applied Sciences 3(3):241–249. https://doi.org/10.1016/j.ejbas.2016.07.005
6. Chojnacka K, Mikulewicz M (2019) Green analytical methods of metals determination in biosorption studies. TrAC, Trends Anal Chem 116:254–265. https://doi.org/10.1016/j.trac.2019.02.013
7. Redha AA (2020) Removal of heavy metals from aqueous media by biosorption. Arab J Basic App Sci 27(1):183–193. https://doi.org/10.1080/25765299.2020.1756177
8. Bashir A, Malik LA, Ahad S, Manzoor T, Bhat MA, Dar GN, Pandith AH (2019) Removal of heavy metal ions from aqueous system by ion-exchange and biosorption methods. Environ Chem Lett 17:729–754. https://doi.org/10.1007/s10311-018-00828-y
9. Hu X, Cao J, Yang H, Li D, Qiao Y, Zhao J, Zhang Z, Huang L (2020) Pb2+ biosorption from aqueous solutions by live and dead biosorbents of the hydrocarbon-degrading strain Rhodococcus sp HX-2. PLOS ONE 15(1):e0226557. https://doi.org/10.1371/journal.pone.0226557
10. Joseph L, Jun BM, Flora JRV, Park CM, Yoon Y (2019) Removal of heavy metals from water sources in the developing world using low-cost materials: a review. Chemosphere 229:142–159. https://doi.org/10.1016/j.chemosphere.2019.04.198
11. Dai Y, Sun Q, Wang W, Lu L, Liu M, Li J, Yang S, Sun Y, Zhang K, Xu J, Zheng W, Gu Z, Yang Y, Gao Y, Chen Y, Zhang X, Gao F, Zhang Y (2018) Utilizations of agricultural waste as adsorbent for the removal of contaminants: a review. Chemosphere 211:235–253. https://doi.org/10.1016/j.chemosphere.2018.06.179
12. Sud D, Mahajan G, Kaur MP (2008) Agricultural waste material as potential adsorbent for sequestering heavy metal ions from aqueous solutions–a review. Biores Technol 99(14):6017–6027. https://doi.org/10.1016/j.biortech.2007.11.064
13. Huang Y (2017) Research progress of wastewater treatment by agricultural wastes as biological adsorbent. App Chem Industry 2:368–372
14. Kuppusamy S, Thavamani P, Megharaj M, Naidu R (2015) Bioremediation potential of natural polyphenol rich green wastes: a review of current research and recommendations for future directions. Environ Technol Innov 4:17–28. https://doi.org/10.1016/j.eti.2015.04.001
15. Negm, N., Hefni, H.H.H., Abd-Elaal, A.A., 2017. Chp.16. Assessment of agricultural wastes as biosorbents for heavy metal ions removal from wastewater, in: Biresaw, G., Mittal, K.L. (Eds.). Surfactants in tribology, Vol. 5. CRC Press, Boca Raton, pp. 465–491. https://doi.org/10.1201/9781315120829
16. Tripathi SM, Chaurasia S (2020) Detection of chromium in surface and groundwater and its bio-absorption using bio-wastes and vermiculite. Eng Sci Technol, an Int J 23:1153–1161. https://doi.org/10.1016/j.jestch.2019.12.002
17. DesMarias TL, Costa M (2019) Mechanisms of chromium-induced toxicity. Curr Opinion Toxicol 14:1–7. https://doi.org/10.1016/j.cotox.2019.05.003
18. Lin Z, Li J, Luan Y, Dai W (2020) Application of algae for heavy metal adsorption: a 20-year meta-analysis. Ecotoxicol Environ Saf 190:110089. https://doi.org/10.1016/j.ecoenv.2019.110089
19. Beres C, Costa GNS, Cabezudo I, da Silva-James NK, Teles ASC, Cruz APG, Mellinger-Silva C, Tonon RV, Cabral LMC, Freitas SP (2017) Towards integral utilization of grape pomace from winemaking process: a review. Waste Manage 68:581–594. https://doi.org/10.1016/j.wasman.2017.07.017
20. Garcia-Jares C, Vazquez A, Lamas JP, Pajaro M, Alvarez-Casas M, Lores M (2015) Antioxidant white grape seed phenolics: pressurized liquid extracts from different varieties. Antioxidants 4(4):737–749. https://doi.org/10.3390/antiox4040737
21. Dimić I, Teslić N, Putnik P, Bursać Kovačević D, Zeković Z, Šojić B, Mrkonjić Ž, Čolović D, Montesano D, Pavlić B (2020) Innovative and conventional valorizations of grape seeds from winery by-products as sustainable source of lipophilic antioxidants. Antioxidants 9:568. https://doi.org/10.3390/antiox9070568
22. Palacios Macías, V., Pérez Rodríguez, L., Nebot Sanz, E., 1997. Aplicación de análisis estadísticos multivariantes al estudio del proceso de maduración de la uva en el marco del Jerez. Servicio de Publicaciones de la Universidad de Cádiz, Cádiz, pp. 210

23. Nogales-Bueno J, Baca-Bocanegra B, Rooney A, Hernández-Hierro JM, Byrne H, Heredia FJ (2017) Study of phenolic extractability in grape seeds by means of ATR-FTIR and Raman spectroscopy. Food Chem 232:602–609. https://doi.org/10.1016/j.foodchem.2017.04.049
24. Antonic B, Janˇcíková S, Dordevic D, Tremlová B (2020) Grape pomace valorization: a systematic review and meta-analysis. Foods 9:1627. https://doi.org/10.3390/foods9111627
25. Pereira MG, Hamerski F, Andrade EF, Scheer AP, Corazza ML (2017) Assessment of subcritical propane, ultrasound-assisted and Soxhlet extraction of oil from sweet passion fruit (*Passiflora alata* Curtis) seeds. The Journal of Supercritical Fluids 128:338–348. https://doi.org/10.1016/j.supflu.2017.03.021
26. Pholosi A, Ofomaja AE, Naidoo EB (2013) Effect of chemical extractants on the biosorptive properties of pine cone powder: Influence on lead(II) removal mechanism. J Saudi Chem Soc 17(1):77–86. https://doi.org/10.1016/j.jscs.2011.10.017
27. Karim, M.R., Rahman, M.A., Miah, M.A.J., Ahmad, H., Yanagisawa, M., Ito, M., 2011. Synthesis of γ-alumina particles and surface characterization. The Open Colloid Science Journal, 2011, 4, 32–36. https://benthamopen.com/contents/pdf/TOCOLLSJ/TOCOLLSJ-4-32.pdf
28. Dopico-Ramírez, D., León-Fernández, V., Díaz-López, C., Peña-Sartorio, E., Céspedes-Sánches, M.I., 2016. Meollo del bagazo: caracterización físico-química y potencialidades como biosorbente de especies catiónicas en solución, ICIDCA. Sobre los Derivados de la Caña de Azúcar 50(2), 29–34. https://www.redalyc.org/articulo.oa?id=223150958005
29. Pakade VE, Ntuli TD, Ofomaja AE (2017) Biosorption of hexavalent chromium from aqueous solutions by *Macadamia* nutshell powder. Appl Water Sci 7:3015–3030. https://doi.org/10.1007/s13201-016-0412-5
30. Statgraphics Centurion XVII, 2014. Data analysis software system, version 17.1.02.
31. Khelaifia FZ, Hazourli S, Nouacer S, Rahima H, Ziati M (2016) Valorization of raw biomaterial waste-date stones-for Cr(VI) adsorption in aqueous solution: thermodynamics, kinetics and regeneration studies. Int Biodeterior Biodegradation 114:76–86. https://doi.org/10.1016/j.ibiod.2016.06.002
32. Turco A, Pennetta A, Caroli A, Mazzotta E, Monteduro AG, Primiceri E, de Benedetto G, Malitesta C (2019) Easy fabrication of mussel inspired coated foam and its optimization for the facile removal of copper from aqueous solutions. J Colloid Interface Sci 552:401–411. https://doi.org/10.1016/j.jcis.2019.05.059
33 Kar S, Equeenuddin SM (2019) Adsorption of hexavalent chromium using natural goethite: isotherm thermodynamic and kinetic study. J Geologic Soc India 93:285–292. https://doi.org/10.1007/s12594-019-1175-z
34. Saha B, Orvig C (2010) Biosorbents for hexavalent chromium elimination from industrial and municipal effluents. Coord Chem Rev 254:2959–2972. https://doi.org/10.1016/j.ccr.2010.06.005
35. Bartczak P, Norman M, Klapiszewski L, Karwańska N, Kawalec M, Baczynska M, Wysokowski M, Zdarta J, Ciesielczyk F, Jesionowski T (2018) Removal of nickel(II) and lead(II) ions from aqueous solution using peat as a low-cost adsorbent: a kinetic and equilibrium study. Arab J Chem 11:1209–1222. https://doi.org/10.1016/j.arabjc.2015.07.018
36. Önal Y (2006) Kinetics of adsorption of dyes from aqueous solution using activated carbon prepared from waste apricot. J Hazard Mater 137(3):1719–1728. https://doi.org/10.1016/j.jhazmat.2006.05.036
37. Davoodi SM, Taheran M, Brara SK, Galvez-Cloutier R, Martel R (2019) Hydrophobic dolomite sorbent for oil spill clean-ups: kinetic modeling and isotherm study. Fuel 251:57–72. https://doi.org/10.1016/j.fuel.2019.04.033
38. Cheung W, Porter JF, Mckay G (2001) Sorption kinetic analysis for the removal of cadmium ions from effluents using bone char. Water Res 35(3):605–612. https://doi.org/10.1016/S0043-1354(00)00306-7
39. Foroutan R, Esmaeili H, Fard MK (2015) Equilibrium and kinetic studies of Pb(II) biosorption from aqueous solution using shrimp peel. Int Res J App Basic Sci 9(11):1954–1965
40. Milmile SN, Pande JV, Karmakar S, Bansiwal A, Chakrabarti T, Biniwale RB (2011) Equilibrium isotherm and kinetic modeling of the adsorption of nitrates by anion exchange Indion NSSR resin. Desalination 276:38–44. https://doi.org/10.1016/j.desal.2011.03.015
41. Yagub MT, Sen TK, Afroze S, Ang HM (2014) Dye and its removal from aqueous solution by adsorption: a review. Adv Coll Interface Sci 209:172–184. https://doi.org/10.1016/j.cis.2014.04.002
42. Ofomaja AE, Naidoo EB, Modise SJ (2010) Surface modification of pine cone powder and its application for removal of Cu(II) from wastewater. Desalin Water Treat 19:275–285. https://doi.org/10.5004/dwt.2010.1230
43. American Water Works Association, AWWA, 1991. Standards for granular activated carbons American Water Works Association, ANSI/AWWA B604–90 Denver Co, USA.
44. Enemose, E.A., Osakwe, S.A., 2014. Effect of metal ion concentration on the biosorption of Al^{3+} and Cr^{6+} by almond tree (*Terminalia catappa L.*) leaves. Chemistry and Materials Research 6(4) 12–17. https://iiste.org/Journals/index.php/CMR/article/view/12151
45. Babalola JO, Olowoyo JO, Durojaiye AO, Olatunde AM, Unuabonah EI, Omorogie MO (2016) Understanding the removal and regeneration potentials of biogenic wastes for toxic metals and organic dyes. J Taiwan Inst Chem Eng 58:490–499. https://doi.org/10.1016/j.jtice.2015.07.003
46. Malik PK (2003) Use of activated carbons prepared from sawdust and rice-husk for adsorption of acid dyes: a case study of Acid Yellow 36. Dyes Pigm 56(3):239–249. https://doi.org/10.1016/S0143-7208(02)00159-6
47. Al-Ghouti MA, Al-Absi RS (2020) Mechanistic understanding of the adsorption and thermodynamic aspects of cationic methylene blue dye onto cellulosic olive stones biomass from wastewater. Sci Rep 10:15928. https://doi.org/10.1038/s41598-020-72996-3
48. Tounsadi H, Khalidi A, Machrouhi A, Farnane M, Elmoubarki R, Elhalil A, Sadiq M, Barka N (2016) Highly efficient activated carbon from Glebiois coronaria L biomass: optimization of preparation conditions and heavy metals removal using experimental design approach. J Environ Chem Eng 4(4):4549–4564. https://doi.org/10.1016/j.jece.2016.10.020
49. Tounsadi H, Khalidi A, Farnane M, Abdennouri M, Barka N (2016) Experimental design for the optimization of preparation conditions of highly efficient activated carbon from *Glebionis coronaria* L. and heavy metals removal ability. Process Saf Environ Prot 102:710–723. https://doi.org/10.1016/j.psep.2016.05.017
50. Rugnini L, Costa G, Congestri R, Antonaroli S, Sanità di Toppi L, Bruno L (2018) Phosphorus and metal removal combined with lipid production by the green microalga *Desmodesmu* sp.: an integrated approach. Plant Physiol Biochem 125:45–51. https://doi.org/10.1016/j.plaphy.2018.01.032

51. Ye L, Zhang J, Zhao J, Luo Z, Tu S, Yin Y (2015) Properties of biochar obtained from pyrolysis of bamboo shoot shell. J Anal Appl Pyrol 114:172–178. https://doi.org/10.1016/j.jaap.2015.05.016
52. Aravindhan R, Raghava Rao J, Unni Nair B (2009) Preparation and characterization of activated carbon from marine macro-algal biomass. J Hazard Mater 162(2–3):688–694. https://doi.org/10.1016/j.jhazmat.2008.05.083
53. Ortíz-Gutiérrez M, Alfaro-Cuevas-Villanueva R, Martínez-Miranda V, Hernández-Cristóbal O, Cortés-Martínez R (2020) Reduction and biosorption of Cr(VI) from aqueous solutions by acid-modified guava seeds: kinetic and equilibrium studies. Pol J Chem Technol 22(4):36–47
54. Lucarini M, Durazzo A, Kiefer J, Santini A, Lombardi-Boccia G, Souto EB, Romani A, Lampe A, Ferrari Nicoli S, Gabrielli P, Bevilacqua N, Campo M, Morassut M, Cecchini F (2020) Grape seeds: chromatographic profile of fatty acids and phenolic compounds and qualitative analysis by FTIR-ATR spectroscopy. Foods 9(1):10. https://doi.org/10.3390/foods9010010
55. Farinella NV, Matos GD, Arruda MAZ (2007) Grape bagasse as a potential biosorbent of metals in effluent treatments. Biores Technol 98(10):1940–1946. https://doi.org/10.1016/j.biortech.2006.07.043
56. Güzel, F., Sayğılı, G.A., Sayğılı, H., Koyuncu, F., Kaya N., Güzel, S., 2020. Performance of grape (*Vitis vinifera L.)* industrial processing solid waste–derived nanoporous carbon in copper(II) removal. Biomass Conversion and Biorefinery. https://doi.org/10.1007/s13399-020-00787-x
57. Zúñiga-Muro NM, Bonilla-Petriciolet A, Mendoza-Castillo DI, Reynel-Ávila HE, Duran-Valle CJ, Ghalla H, Sellaoui L (2020) Recovery of grape waste for the preparation of adsorbents for water treatment: mercury removal. J Environ Chem Eng 8(3):103738. https://doi.org/10.1016/j.jece.2020.103738
58. Albadarin AB, Mangwandi C, Walker GM, Allen SJ, Mohammad NM, Ahmad MNM, Khraisheh M (2013) Influence of solution chemistry on Cr(VI) reduction and complexation onto date-pits/tea-waste biomaterials. J Environ Manage 114:190–201. https://doi.org/10.1016/j.jenvman.2012.09.017
59. Dos Santos VCG, Salvado APA, Dragunski DC, Peraro DNC, Tarley CRT (2012) Highly improved chromium(III) uptake capacity in modified sugarcane bagasse using different chemical treatments. Quim Nova 35(8):1606–1611. https://doi.org/10.1590/S0100-40422012000800021
60. Rosales E, Escudero S, Pazos M, Sanromán MA (2019) Sustainable removal of Cr(VI) by lime peel and pineapple core wastes. Appl Sci 9(10):1967. https://doi.org/10.3390/app9101967
61. Welch CM, Nekrassova O, Compton RG (2005) Reduction of hexavalent chromium at solid electrodes in acidic media: reaction mechanism and analytical applications. Talanta 65(1):74–80. https://doi.org/10.1016/j.talanta.2004.05.017
62. Stern CM, Jegede TO, Hulse VA, Elgrishi N (2021) Electrochemical reduction of Cr(VI) in water: lessons learned from fundamental studies and applications. Chem Soc Rev 50:1642–1667. https://doi.org/10.1039/D0CS01165G
63. Ramsey JD, Xia L, Kendig MW, McCreery RL (2001) Raman spectroscopic analysis of the speciation of dilute chromate solutions. Corros Sci 43(8):1557–1572. https://doi.org/10.1016/S0010-938X(00)00145-1
64. Pujol D, Liu C, Fiol N, Olivella MA, Gominho J, Villaescusa I, Pereira H (2013) Chemical characterization of different granulometric fractions of grape stalks waste. Ind Crops Prod 50:494–500. https://doi.org/10.1016/j.indcrop.2013.07.051
65. Kurniawan A, Sisnandy VOA, Trilestari K, Sunarso J, Indraswate N, Ismadji S (2011) Performance of durian shell waste as high capacity biosorbent for Cr(VI) removal from synthetic wastewater. Ecol Eng 37(6):940–947. https://doi.org/10.1016/j.ecoleng.2011.01.019
66. Ben Khalifa E, Rzig B, Chakroun R, Nouagui H, Hamrouni B (2019) Application of response surface methodology for chromium removal by adsorption on low-cost biosorbent. Chemom Intell Lab Syst 189:18–26. https://doi.org/10.1016/j.chemolab.2019.03.014
67. Ogata F, Nagai N, Itami R, Nakamura T, Kawasaki N (2020) Potential of virgin and calcined wheat bran biomass for the removal of chromium(VI) ion from a synthetic aqueous solution. J Environ Chem Eng 8(2):103710. https://doi.org/10.1016/j.jece.2020.103710
68. Hariharan, A., Harini, V., Sandhya, S. et al., 2020. Waste *Musa acuminata* residue as a potential biosorbent for the removal of hexavalent chromium from synthetic wastewater. Biomass Conversion and Biorefinery, published on line 25 November. https://doi.org/10.1007/s13399-020-01173-3
69. Akram M, Bhatti HN, Iqbal M, Noreen S, Sadaf S (2017) Biocomposite efficiency for Cr(VI) adsorption: kinetic, equilibrium and thermodynamics studies. J Environ Chem Eng 5(1):400–411. https://doi.org/10.1016/j.jece.2016.12.002
70. Saravanan A, Kumar PS, Vo DVN, Swetha S, Tsopbou Ngueagni P, Karishma S, Jeevanantham S, Yaashikaa PR (2021) Ultrasonic assisted agro waste biomass for rapid removal of Cd(II) ions from aquatic environment: mechanism and modelling analysis. Chemosphere 271:129484. https://doi.org/10.1016/j.chemosphere.2020.129484
71. Tadesse B, Teju E, Megersa N (2015) The Teff straw: a novel low-cost adsorbent for quantitative removal of Cr(VI) from contaminated aqueous samples. Desalin Water Treat 56(11):2925–2936. https://doi.org/10.1080/19443994.2014.968214
72. Prasanthi MR, Jayasravanthi M, Nadh RV (2016) Kinetic, thermodynamic and equilibrium studies on removal of hexavalent chromium from aqueous solutions using agro-waste biomaterials, casuarina equisetifolia L. and sorghum bicolor. Korean J Chem Eng 33(8):2374–2383. https://doi.org/10.1007/s11814-016-0078-6
73. Ding D, Ma X, Shi W, Lei Z, Zhang Z (2016) Insights into mechanisms of hexavalent chromium removal from aqueous solution by using rice husk pretreated using hydrothermal carbonization technology. Royal Soc Chem Advances 6:74675–74682. https://doi.org/10.1039/c6ra17707g
74. Hyder AHMG, Begum SA, Egiebor NO (2015) Adsorption isotherm and kinetic studies of hexavalent chromium removal from aqueous solution onto bone char. J Environ Chem Eng 3:1329–1336. https://doi.org/10.1016/j.jece.2014.12.005
75. Rangabhashiyam S, Balasubramanian P (2018) Adsorption behaviors of hazardous methylene blue and hexavalent chromium on novel materials derived from Pterospermum acerifolium shells. J Mol Liq 254(2018):433–445. https://doi.org/10.1016/j.molliq.2018.01.131
76. Rangabhashiyam S, Sayantani S, Balasubramanian P (2019) Assessment of hexavalent chromium biosorption using biodiesel extracted seeds of Jatropha sp., Ricinus sp. and Pongamia sp. Int J Environ Sci Technol 16:5707–5724. https://doi.org/10.1007/s13762-018-1951-0
77. Zhang Y, Wan H, Zhao J, Li J (2019) Biosorption of anionic and cationic dyes via raw and chitosan oligosaccharide-modified *Huai Flos Chrysanthemum* at different temperatures. RCS Advances 9:11202–11211. https://doi.org/10.1039/C9RA00378A
78. Abdolali, A., Ngo, H.H., Guo, W., Lu, S., Chen, S., Nguyen, N.C., Zhang, X., Wang, J., Wu, Y., 2016. A breakthrough biosorbent in removing heavy metals: equilibrium, kinetic, thermodynamic and mechanism analyses in a lab-scale study. Science of The Total Environment 542, Part A, 603–611. https://doi.org/10.1016/j.scitotenv.2015.10.095

79. Horsfall M.J., Spiff, A., 2005. Effects of temperature on the sorption of Pb^{2+} and Cd^{2+} from aqueous solution by *Caladium bicolor* (Wild Cocoyam) biomass. Electronic Journal of Biotechnology 8(2), 43–50. https://scielo.conicyt.cl/pdf/ejb/v8n2/a05.pdf
80. Baral SS, Das N, Chaudhury GR, Das SN (2009) A preliminary study on the adsorptive removal of Cr(VI) using seaweed Hydrilla verticillata. J Hazard Mater 171(1–3):358–369. https://doi.org/10.1016/j.jhazmat.2009.06.011
81. Antony GS, Manna A, Baskaran S, Puhazhendi P, Ramchary A, Niraikulam A, Ramudu KN (2020) Non-enzymatic reduction of Cr(VI) and it's effective biosorption using heat-inactivated biomass: a fermentation waste material. J Hazard Mater 392:122257. https://doi.org/10.1016/j.jhazmat.2020.122257
82. Ding D, Ma X, Shi W, Lei Z, Zhang Z (2016) Insights into mechanisms of hexavalent chromium removal from aqueous solution by using rice husk pretreated using hydrothermal carbonization technology. RSC Adv 6:74675–74682. https://doi.org/10.1039/C6RA17707G
83. Li Y, Yue QY, Gao BY (2010) Effect of humic acid on the Cr(VI) adsorption onto Kaolin. Appl Clay Sci 48:481–484. https://doi.org/10.1016/j.clay.2010.02.010
84. Gupta A, Balomajumder C (2015) Biosorptive performance of *Escherichia coli* supported on Waste tea biomass (WTB) for removal of Cr(VI) to avoid the contamination of ground water: a comparative study between biosorption and SBB system. Groundw Sustain Dev 1(1–2):12–22. https://doi.org/10.1016/j.gsd.2016.01.001
85. El-Naggar NEA, El-khateeb AY, Ghoniem AA, El-Hersh MS, WesamEldin IA, Saber WIA (2020) Innovative low-cost biosorption process of Cr^{6+} by *Pseudomonas alcaliphila* NEWG-2. Sci Rep 10:14043. https://doi.org/10.1038/s41598-020-70473-5